1-6-2006

Second order nonlinear inelastic analysis of composite steel–concrete members. II: applications

Y. L. Pi
University of New South Wales

M. A. Bradford
University of New South Wales

B. Uy
University of Wollongong, brianuy@uow.edu.au

Second Order Nonlinear Inelastic Analysis of Composite Steel–Concrete Members. II: Applications

Yong-Lin Pi[1]; Mark Andrew Bradford, M.ASCE[2]; and Brian Uy, M.ASCE[3]

Abstract: In the companion paper, a total Lagrangian finite element (FE) model was formulated for the second order nonlinear inelastic analysis of steel–concrete composite members. This paper describes the implementation of the incremental–iterative procedure for the FE model. It has been found that using the standard tangent modulus matrix in an incremental–iterative solution procedure may cause error accumulations. These errors in turn lead to an unsafe drift from the yield surfaces, and the yield criteria may be violated. Consequently, the quadratic asymptotic rate of convergence of the Newton–Raphson method is lost. To solve this problem, a consistent tangent modulus matrix is needed in the incremental–iteration solution process, and this is described. This paper presents the implementation of the FE model and shows how to use the constitutive models in the companion paper in association with the uniaxial stress–strain relations including that for confined concrete. Some of the applications of the FE model to various problems are also shown in this paper. The comparisons between numerical and experimental results demonstrate that the FE model provides excellent numerical performance for the nonlinear inelastic analysis of steel–concrete composite members.

DOI: 10.1061/(ASCE)0733-9445(2006)132:5(762)

CE Database subject headings: Beams; Columns; Composite materials; Inelastic action; Concrete; Steel; Finite element method.

Introduction

In the companion paper (Pi et al. 2006), a total Lagrangian finite element (FE) model for the second order nonlinear inelastic analysis of composite members was formulated. The total deformation was assumed to result from two successive motions: displacements and finite rotations of the cross section, and a superimposed relative slip displacement between the steel and concrete components in the deformed configuration. The relative slip between the steel and concrete components due to flexible bond at the interface between the steel and concrete components is considered as an independent displacement in the formulation. The shear strains and shear stresses produced by the interaction between the slip and the in-plane bending are included in the FE model. The second order nonlinear equilibrium equations of the FE model are usually solved by an incremental–iterative procedure associated with Newton–Raphson methods, which is presented in this paper.

In the companion paper, the criteria for the yield of the steel, the yield of the concrete in the compressive zone, the cracking of the concrete in the tensile zone, and the crushing of the compressive concrete were stated. The incremental relationships between the increments of the stresses and strains were also established. These relationships can be used to compute the increments of stresses from the increments of strains and are suitable only for infinitesimal increments of the stresses and strains. However, it is known that the increments of the strains obtained in an incremental–iterative procedure are not infinitesimally small. Replacing the infinitesimal increments of strains and stresses by the small finite increments may lead to error accumulations in the incremental–iterative procedure that is used. These errors may then lead to an unsafe drift from the yield surface and the yield criterion may be violated. Consequently, the quadratic asymptotic rate of convergence of the Newton–Raphson method is lost. This paper discusses a technique to overcome this difficulty.

In addition, the constitutive models for steel, concrete, and slip at the interface need to be used in association with uniaxial stress–strain relations. The stress–strain relations are dependent on the material, the location of the element, and confinement effects. For example, the slip stiffness at the connections is different from the other part of CFT columns. The stress–strain curve for confined concrete is different from that for unconfined concrete. Therefore, the stress–strain relations need to be assign to each element in the FE implementation in accordance with the material, the confinement, and location of the element.

As pointed out in the companion paper, a generic or unified FE model that is suitable for all types of composite steel concrete members; viz. simply supported beams, continuous composite beams, and concrete filled steel tube columns does not appear to have been reported. This paper demonstrates the excellent numerical performance of the FE model for the nonlinear inelastic analysis of a variety of problems encountered in composite structures.

[1]Senior Research Fellow, School of Civil & Environmental Engineering, Univ. of New South Wales, Sydney, NSW 2052, Australia. E-mail: y.pi@unsw.edu.au

[2]Professor, School of Civil & Environmental Engineering, Univ. of New South Wales, Sydney, NSW 2052, Australia (corresponding author). E-mail: m.bradford@unsw.edu.au

[3]Professor, School of Civil & Mining Engineering, The Univ. of Wollongong, Wollongong, NSW 2500, Australia. E-mail: brianuy@uow.edu.au

Note. Associate Editor: Sherif El-Tawil. Discussion open until October 1, 2006. Separate discussions must be submitted for individual papers. To extend the closing date by one month, a written request must be filed with the ASCE Managing Editor. The manuscript for this paper was submitted for review and possible publication on April 20, 2004; approved on June 27, 2005. This paper is part of the ***Journal of Structural Engineering***, Vol. 132, No. 5, May 1, 2006. ©ASCE, ISSN 0733-9445/2006/5-762–771/$25.00.

Implementation

General

The incremental–iterative FE model formulated in the companion paper is applied to various problems and the solutions are compared with existing theoretical and experimental results in this paper. In the implementation of the incrementations and iterations of the FE model, each load step consists of the application of an increment of external loads and subsequent iterations to restore equilibrium. Before the restoration, the internal and external forces are not in equilibrium and hence the virtual work dU does not vanish, and 1 the incremental–iterative equilibrium equations can be written as

$$\mathbf{k}_i \Delta \mathbf{r}_i^j = \Delta \mathbf{p}_i + \Delta \mathbf{p}_i^{j-1} \tag{1}$$

where i and j denote the load step and the iteration within the load step, respectively, and $\Delta \mathbf{p}_i^{j-1}$ = unbalanced force in the last iteration $(j-1)$ that can be calculated using (Pi et al. 2006)

$$\Delta \mathbf{p}_i^{j-1} = \left\{ \int_0^l \mathbf{N}^T (\mathbf{B}^T \mathbf{R} + \mathbf{q}_{\text{sh}}) dz - \int_0^l \mathbf{N}^T \mathbf{A}^T \mathbf{q} dz - \sum_{k=1,2} \mathbf{N}^T \mathbf{A}^T \mathbf{Q}_k \right\}_i^{j-1} \tag{2}$$

The arc-length method is used as the iterative strategy and the automatic incrementation of the arc length is adopted (Crisfield 1986). The sign of the load increment follows the sign of the determinant of the tangent stiffness matrix. A convergence criterion based on the maximum norm of the incremental displacements is adopted.

Strain Updating

Two different methods can be used for updating the strains. The first method is to use the incremental strains, which uses the increments of the general displacements given by (Pi et al. 2006)

$$\Delta \boldsymbol{\theta}_i^j = \Delta \boldsymbol{\theta}_i^{j-1} + \delta \boldsymbol{\theta}_i^j \tag{3}$$

where the generalized displacements $\boldsymbol{\theta}$ are given by

$$\boldsymbol{\theta} = \{u', u'', u''', v', v'', v''', w', \phi, \phi', \phi'', \Omega, \Omega'\}^T \tag{4}$$

and $\delta \boldsymbol{\theta}_i^j$ = current iterative displacement vector at the Gauss points of the elements along the beam.

The strain increments are then obtained as

$$\Delta \boldsymbol{\epsilon}_i^j = \mathbf{S}\mathbf{B}_i \Delta \boldsymbol{\theta}_i^j \tag{5}$$

The stress increments and stresses at the iteration j can then be calculated from the strain increments $\Delta \boldsymbol{\epsilon}_i^j$. The incremental equations given by Eq. (44) in Part I for steel and given by Eq. (64) in Part I for compressive behavior of concrete in the companion paper (Pi et al. 2006) can written as

$$d\boldsymbol{\sigma} = \mathbf{E}(\mathbf{I} - \mathbf{a}\mathbf{c}^T) d\boldsymbol{\epsilon} = \mathbf{E}^{(\text{ep})} d\boldsymbol{\epsilon} \tag{6}$$

with the elastic–plastic tangent modulus material matrix $\mathbf{E}^{(\text{ep})}$ being

$$\mathbf{E}^{(\text{ep})} = \mathbf{E}(\mathbf{I} - \mathbf{a}\mathbf{c}^T) \tag{7}$$

Eq. (6) is accurate only for infinitesimal increments of the strains $d\boldsymbol{\epsilon}$ and infinitesimal increments of the stresses $d\boldsymbol{\sigma}$. However, the strain increments obtained from Eq. (5) are not necessarily infinitesimally small.

Replacing the infinitesimal increments $d\boldsymbol{\epsilon}$ and $d\boldsymbol{\sigma}$ in Eq. (6) with the finite but small increments $\Delta\boldsymbol{\epsilon}$ and $\Delta\boldsymbol{\sigma}$ may lead to error accumulations in the incremental–iterative procedure. These errors may lead to an unsafe drift from the yield surface and the yield criterion may be violated, and so the quadratic asymptotic rate of convergence of the Newton–Raphson method is lost. To solve this problem, a consistent tangent modulus matrix (Simo and Taylor 1985) is needed in the iteration process, instead of the standard tangent modulus matrix $\mathbf{E}^{(\text{ep})}$. The consistent tangent modulus matrix is given by

$$\mathbf{E}_c^{(\text{ep})} = \Omega - \frac{\Omega \mathbf{a}\mathbf{a}^T \Omega^T}{H' + \mathbf{a}^T \Omega \mathbf{a}} \tag{8}$$

where matrix Ω is given by

$$\Omega = \mathbf{P}^{-1}\mathbf{E}$$

and

$$\mathbf{P} = \mathbf{I} + d\lambda \mathbf{E} \frac{\partial \mathbf{a}}{\partial \boldsymbol{\sigma}} \tag{9}$$

and $d\lambda$ = plastic multiplier. Using this method can avoid "spurious unloading" during the iterations.

Alternatively, a subincrement technique can be used to reduce the errors that are introduced. However, using subincrements may increase the total number of iterations within an increment because the same number of subincrements is needed for the later as well as for the earlier iterations, even though the iterative strains will be considerably small.

The second method is to use the iterative strains. In this method, the strain increments are obtained by using the iterative displacements

$$\delta \boldsymbol{\epsilon}_i^j = \mathbf{S}\mathbf{B}_i \delta \boldsymbol{\delta}_i^j \tag{10}$$

Because the iterative strains can be considered to be infinitesimally small, the rate Eq. (6) and the standard tangent modulus matrix given by Eq. (7) can be used and subincrements may not be needed. However, this method may again lead to "spurious unloading" during the iteration. To avoid spurious unloading, "incremental reversibility" can be used in the iteration process. In this technique, a point which deforms plastically during an increment is assumed to unload plastically until the plastic work done again becomes equal to its value at the beginning of the increment considered.

Division and Sampling Points Scheme for Cross Section

A composite cross section needs to be divided into several components so as to use the corresponding material properties and constitutive models in the most appropriate way. The composite

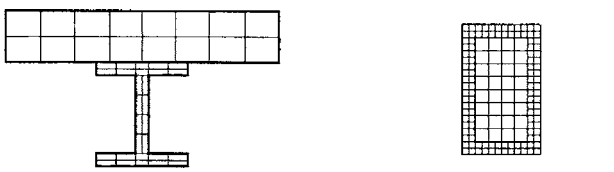

(a) Composite steel-concrete beams (b) Concrete-filled steel tubes

Fig. 1. Division and integration scheme over cross section

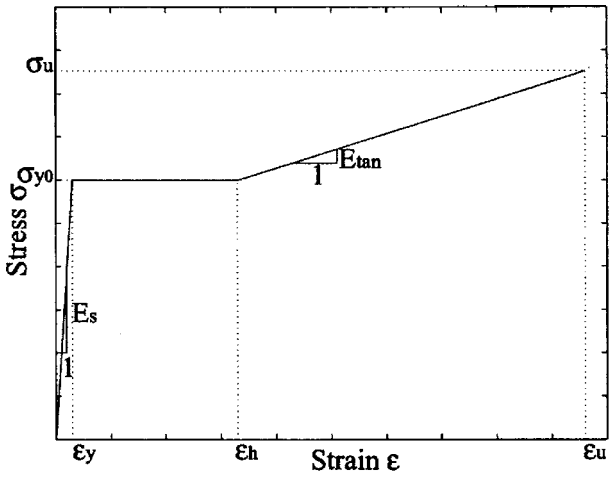

(a) Tri-linear stress-strain curve

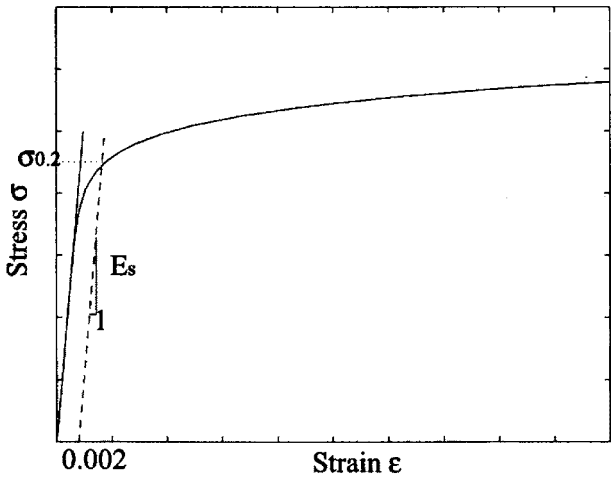

(b) Ramberg-Osgood stress-strain curve

Fig. 2. Stress–strain curve for steel

steel–concrete open section can be divided into four components: the concrete slab, reinforcement, steel deck sheeting, and steel beam or into three components: the concrete slab, reinforcement, and steel beam. CFT columns can be divided into steel tube and concrete core.

The accuracy of the incremental–iterative plastic analysis is related not only to the algorithm used, but also to the sampling point scheme over the cross section that should be chosen in the most appropriate way. In order to determine the correct stress state over the entire cross section and to detect the cracking and crushing of the concrete correctly, the sampling point scheme shown in Fig. 1 is used in conjunction with the present FE model. Each of the components of the composite cross section are further divided into a number of areas as shown in Fig. 1(a) for composite beams and in Fig. 1(b) for CFT columns. The nonbias Gaussian numerical integration technique (Zienkiewicz and Taylor 1989) is used in the present FE model. The number of areas and the number of Gaussian points in each area can be determined in accordance with the problem at hand.

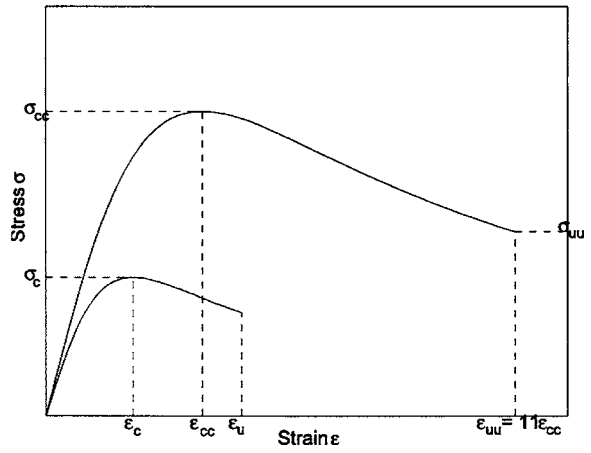

Fig. 3. Stress–strain curve for compressive behavior of concrete

Applications

General

For elasto–plastic analysis, the constitutive equations for the steel, concrete, and shear connectors need to be used in association with their uniaxial stress–strain curves of the corresponding material. Hence, it is important to choose proper uniaxial stress–strain curves. For example, in the CFT columns, the stress–strain curve for confined concrete may need to be used for the concrete core. The trilinear elastic–plastic–strain hardening stress–strain curve shown in Fig. 2(a) is used for the hot-rolled steel component of composite members, where E_s is the Young's modulus of elasticity of the steel, σ_{y0} is the steel yield stress, and ϵ_y is the strain at which the yielding occurs. After onset of yielding, the steel is assumed to be fully plastic until strain hardening starts at the strain ϵ_{hd} which is assumed to be 11 times the yield strain ϵ_y. E_{tan} is the tangent modulus during strain hardening, while the maximum strain ϵ_{max} is assumed to be 31 times the yield strain ϵ_y. These values are typically used by other researchers.

Reinforcement and profiled steel deck sheeting are often used in the concrete slab of composite steel–concrete members and cold-formed tubes are often used for CFT columns. In these cases, the rounded stress and strain curves for display are not typical yield characteristics. In this investigation, the rounded stress–

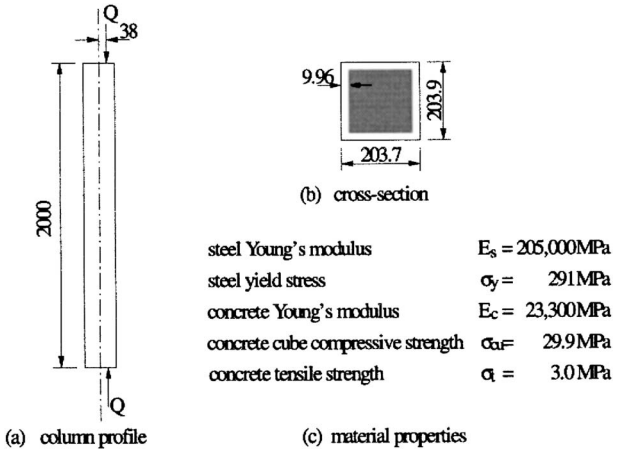

Fig. 4. Concrete-filled steel box column tested by Bridge (1976)

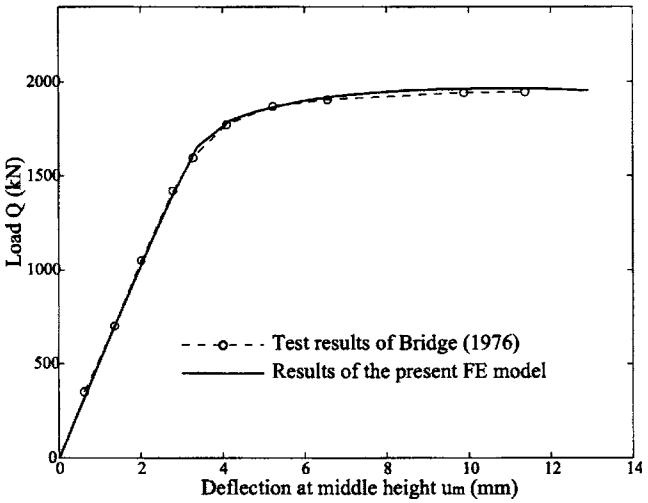

Fig. 5. Comparison with test results of Bridge (1976)

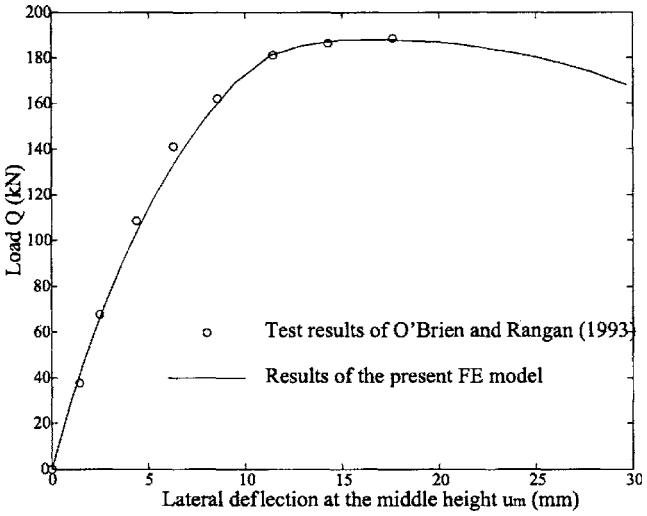

Fig. 7. Comparison with test results of O'Brien and Rangan (1993)

strain curves proposed by Ramberg and Osgood shown in Fig. 2(b) are used for the cold-formed tubes, the steel reinforcement, and profiled deck sheeting, which can be expressed as (Lemaitre and Chaboche 1994)

$$\epsilon = \frac{\sigma}{E_s} + \frac{p}{100}\left(\frac{\sigma}{\sigma_p}\right)^n \tag{11}$$

where E_s=Young's modulus of elasticity; σ_p=reference stress and usually takes the value of the 0.2% proof stress; i.e., $\sigma_p=\sigma_{0.2}$; and the parameters p and n are chosen to match the experimental data.

The stress–strain curve for the compressive behavior of the concrete component of composite members is nonlinear. A large number of empirical stress–strain relationships represented by prescriptive equations have been proposed. The following stress–strain equation proposed by Saenz (1964) is used in this investigation to describe the nonlinear compressive behavior of concrete

$$\sigma = \frac{E_c\epsilon}{1 + (E_c/E_{\text{scnt}} - 2)\epsilon/\epsilon_c + (\epsilon/\epsilon_c)2}. \tag{12}$$

where σ=stress; ϵ=strain; E_c=Young's modulus of elasticity of the concrete; E_{scnt}=secant modulus corresponding to the maximum stress σ_c and given by $E_{\text{scnt}}=\sigma_c/\epsilon_c$, the maximum stress σ_c takes the value of the concrete cylinder compressive strength; and ϵ_c=strain corresponding to the maximum stress σ_c. The stress–strain curve given by this equation shown in Fig. 3 can represent the ascending and descending portions of the nonlinear relationship between the stresses and strains for the concrete component, and is consistent with many other empirical curves.

It can be seen from Eq. (12) that to define a stress–strain curve, the Young's modulus of elasticity of the concrete E_c, the compressive strength of the concrete σ_c, and the corresponding strain ϵ_c are essential. However, in a number of reported experimental studies, these values are not necessarily given. For these cases, in order to use Eq. (12) in the FE analysis for the nonlinear stress–strain behavior of the concrete, the following assumptions and considerations are made. When the value of the cylinder compressive stress σ_c is not available, the cube strength σ_{cu} may be available and then the cylinder compressive stress σ_c is assumed to be given by (Oehlers and Bradford 1995)

$$\sigma_c = 0.85\sigma_{cu} \tag{13}$$

When the Young's modulus of elasticity is not available, its value is assumed to be given by (Warner et al. 1998)

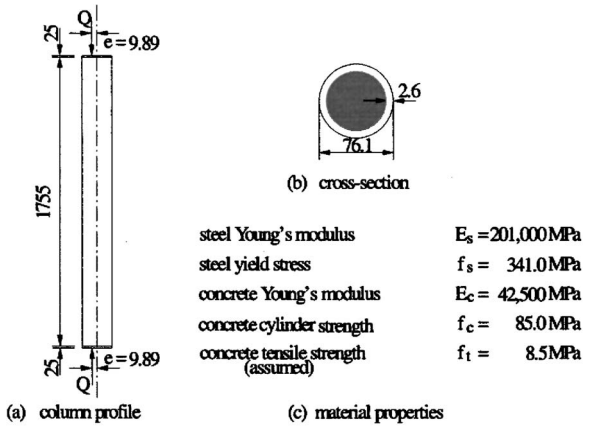

Fig. 6. High strength concrete-filled circular hollow section column tested by O'Brien and Rangan (1993)

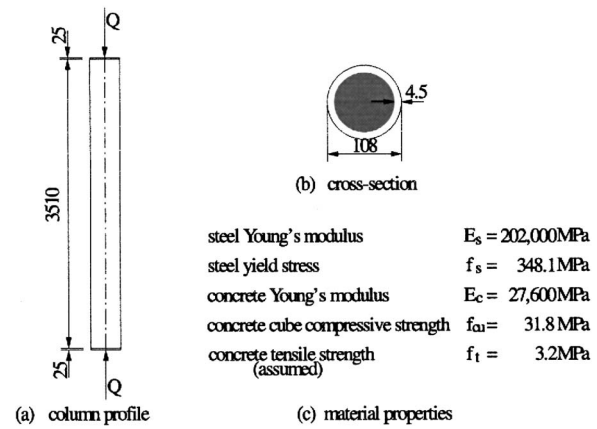

Fig. 8. Concrete-filled circular hollow section column tested by Han (2000)

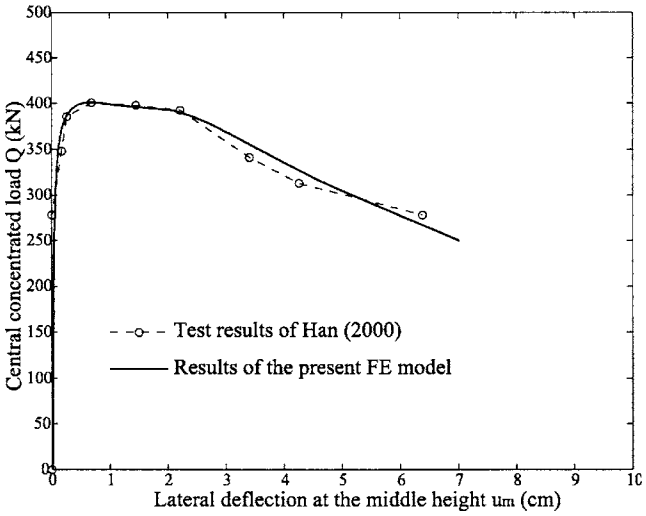

Fig. 9. Comparison with test results of Han (2000)

$$E_c = 0.043\rho^{1.5}\sqrt{\sigma_c} \tag{14}$$

where σ_c and E_c are expressed in MegaPascal and ρ=density of the concrete in kilogram/meter^3. When the density ρ is not available, ρ=2,400 kg/m^3 is assumed. When the value of the strain ϵ_c corresponding to the maximum stress of the concrete is not available, its value is assumed to be (Oehlers and Bradford 1995; Warner et al. 1998)

$$\epsilon_c = 0.002 \tag{15}$$

When confinement effects of the steel tube on the concrete core need to be considered such as in the short CFT columns, the following stress–strain curve shown in Fig. 3 is used

$$\sigma = \frac{E_{cc}\epsilon}{1 + (E_{cc}/E_{scntc} - 2)\epsilon/\epsilon_{cc} + (\epsilon/\epsilon_{cc})^2} \tag{16}$$

where the secant modulus E_{scntc} corresponding to the maximum stress σ_{cc} is given by

$$E_{scntc} = \sigma_{cc}/\epsilon_{cc} \tag{17}$$

in which σ_{cc} and ϵ_{cc}=maximum stress and strain including the confinement effects and given by (Huang et al. 2002)

$$\sigma_{cc} = \sigma_c + k_1\sigma_f \tag{18}$$

and

$$\epsilon_{cc} = \epsilon_c\left(1 + k_2\frac{\sigma_f}{\sigma_c}\right) \tag{19}$$

The values of coefficients k_1 and k_2 can be obtained by calibration from experiments and numerical studies and are assumed to be given Richard et al. (1928) by k_1=4.1 and k_2=20.5 for the CFT column examples in this investigation. The value of the strain ϵ_{uu} (Fig. 3) at which the concrete crashes is assumed to be $\epsilon_{uu}=11\epsilon_{cc}$ (Huang et al. 2002). The stress–strain curve is terminated at $\sigma_{uu}=k_3\sigma_c$. The values of σ_f and k_3 depend on the width-to-thickness ratio and shape of the cross section and so can be determined by matching the numerical results with experimental results via parametric study.

Young's modulus of elasticity of the concrete including the confinement effects of the steel tube is given by (Hu et al. 2003)

$$E_{cc} = 0.043\rho^{1.5}\sqrt{\sigma_{cc}} \tag{20}$$

The tension stiffening phenomenon (Gilbert and Warner 1978) is considered for the tensile behavior of concrete, because tensile stresses are generated in the concrete beyond a crack due to the restraining action by the steel component and the transfer of stresses from the reinforcement and the adjacent uncracked concrete. The bilinear stress–strain curve is used to represent the tensile behavior of the concrete where the Young's modulus of elasticity is the same as that for the compressive behavior, σ_t is the tensile strength of the concrete, and ϵ_{tu} is the maximum tensile strain. The value of the tensile strength σ_t can be obtained from splitting tests. In the absence of reported values, the value of σ_t is assumed to be given by

$$\sigma_t = 0.1\sigma_c \tag{21}$$

The strain ϵ_t corresponding to the tensile strength is $\epsilon_t=\sigma_t/E_c$. The ratio ϵ_{tu}/ϵ_t of the maximum tensile strain to the strain σ_t is

Table 1. Properties of Continuous Beams Tested by Ansourian (1981)

Beam	CTB1	CTB4
Number of studs (19 mm × 75 mm)	66	84
Percentage shear connection	150 (Sagging)	150 (Sagging)
	160 (Hogging)	130 (Hogging)
Longitudinal reinforcement (mm^2)	800 (Hog top)	804 (Hog top)
	316 (Hog bottom)	767 (Hog bottom)
		160 (Sag top)
	160 (Sag bottom)	160 (Sag bottom)
Concrete cube strength (MPa)	30	34
Concrete density (kg/m^3)	2,310	2,280
Yield stress (MPa)		
Flange	277	236
Web	340	238
Reinforcement	430	430
Strain at onset of strain-hardening	0.012	0.018
Initial strain-hardening modulus (MPa)	6,000	3,000

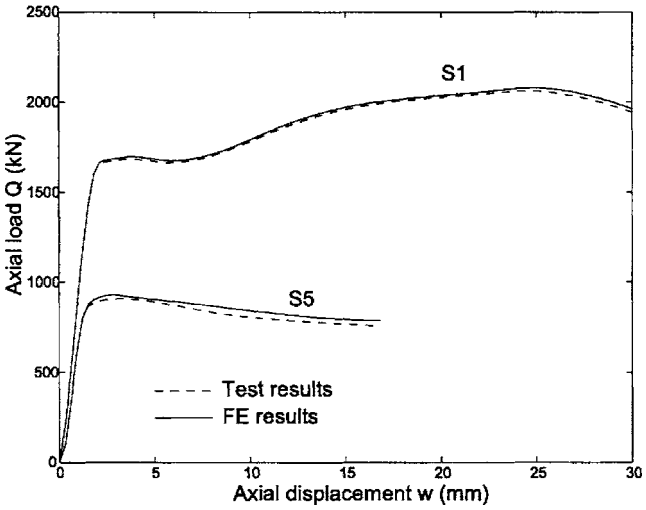

Fig. 10. Comparison with test results of Schneider (1988)

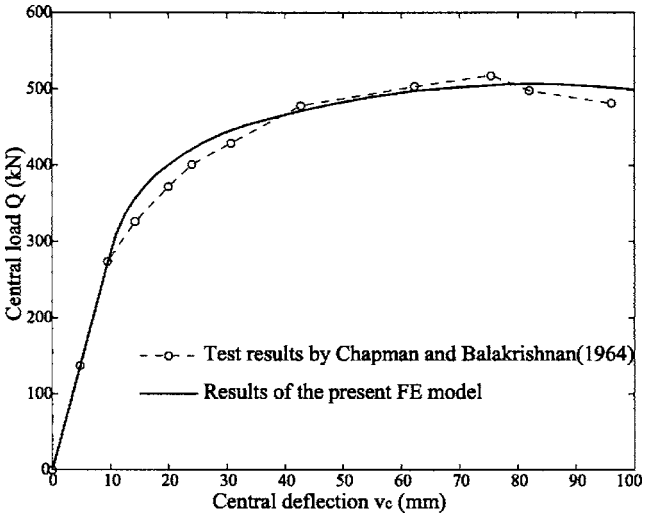

Fig. 12. Comparison with test results for simply supported composite steel–concrete beam of Chapman and Balakrishnan (1964)

chosen to be inversely proportional to the length of the finite element to avoid mesh dependence.

Axial Compression and Uniaxial Bending of Concrete-Filled Box Section Column

Bridge (1976) tested eight concrete-filled box steel columns that were subjected to equal end axial eccentric compressive load so that the columns were bent in symmetric single curvature. The present FE model was used to analyze the specimen SHC-1. The geometric and material properties of the column are shown in Fig. 4. Young's modulus of elasticity E_s=205,000 MPa, suggested by Bridge (1976), was used in the present FE analysis. Variations of the lateral deflections u_m at the middle height of the column with the applied load Q obtained by the present FE model are compared with the test results of Bridge (1976) in Fig. 5. Four elements were used in the FE analysis. It can be seen that the agreement between the FE and test results is very good.

Axial Compression and Uniaxial Bending of High Strength Concrete-Filled CHS Column

O'Brien and Rangan (1993) reported an experimental study on slender tubular steel columns filled with high-strength concrete. The columns were subjected to equal end eccentric compressive load. Nine columns were tested. The present FE model was used to analyze the load–displacement response of the specimen column Number 10 (the specimens were numbered from Number 10 to 18). The geometric and material properties of the column are shown in Fig. 6. Because the strain corresponding to the maximum concrete stress was not reported by O'Brien and Rangan (1993), the value of 0.0035 was assumed for this strain, as this is more representative for high strength concrete than Eq. (15). Variations of the deflection u_m at the middle height of the column with the applied load Q are compared with the test results in Fig. 7. Four elements were used in the FE analysis. Excellent agreement between the FE and test results can be seen from this figure.

Buckling of Slender Concrete-Filled CHS Column

Han (2000) performed tests on 15 slender concrete-filled steel circular hollow section columns that were subjected to equal end central axial compressive load. Some very slender columns buckled when stresses in the steel section were elastic while other columns buckled after yielding of the steel section started. Specimen SC130-2 was chosen for the present FE analysis. The dimensions and the material properties of the column are shown in Fig. 8. Variations of the deflections u_m at the middle height of the

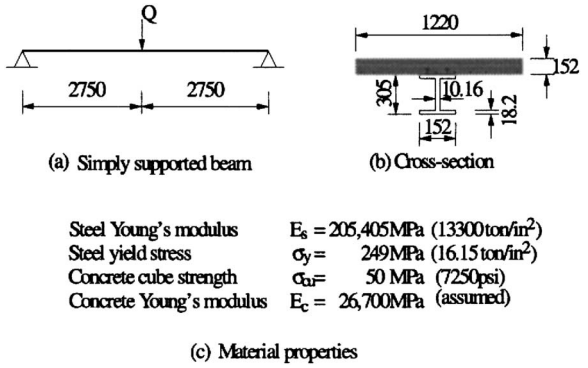

Fig. 11. Simply supported composite steel–concrete beam tested by Chapman and Balakrishnan (1964)

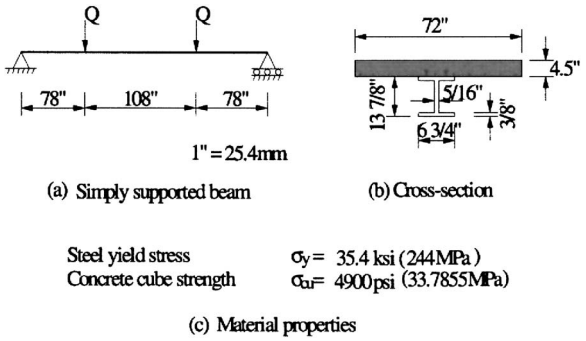

Fig. 13. Simply supported composite steel–concrete beam tested by McGarraugh and Baldwin (1971)

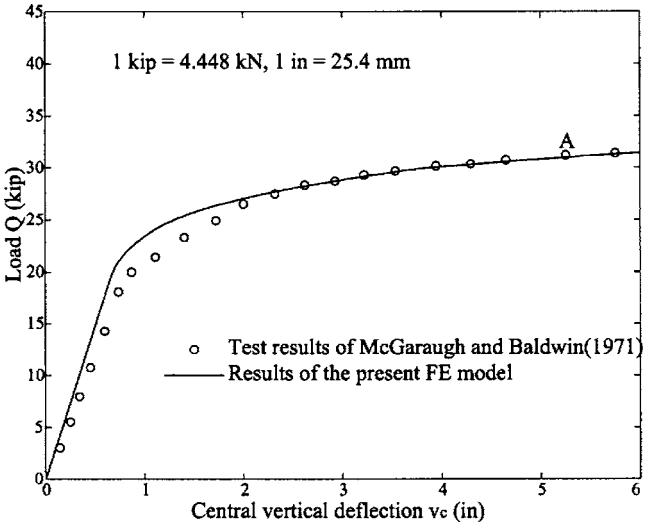

Fig. 14. Load–displacement response compared with test results for simply supported composite steel–concrete beam of McGarraugh and Baldwin (1971)

column with the applied load Q are compared with the test results in Fig. 9. Four elements were used in the FE analysis. The FE results agree with the test results very well.

Axial Compression of Short CFT Columns

Schneider (1988) presented his experimental results on the behavior of short CFT columns concentrated on loading in compression to failure. Three CHS CFT, 5 SHS CFT, and 6 RHS CFT columns were tested. The effects of confinement of the steel tube to the concrete core were reported. The present FE model was used to analyze the load–displacement response of the specimen Column S1 and S5. The geometric and material properties of the column are shown in Table 1. Variations of the axial displacement w with the applied load Q are compared with the test results in Fig. 10. Four elements were used in the FE analysis. The FE results agree with the test results very well.

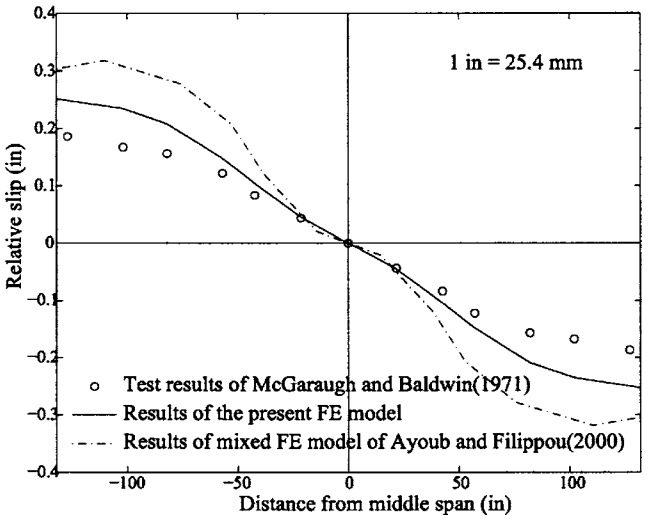

Fig. 15. Slip distribution compared with test results for simply supported composite steel–concrete beam of McGarraugh and Baldwin (1971) at load level A

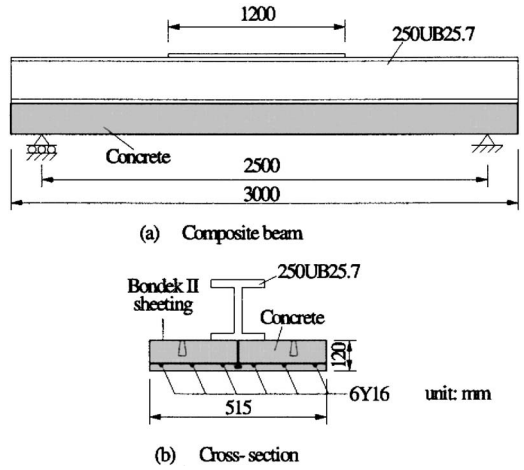

Fig. 16. Simply supported composite steel–concrete in hogging bending beam tested by Loh et al. (2004)

Simply Supported Composite Beam Tested by Chapman and Balakrishnan

Chapman and Balakrishnan (1964) tested 17 simply supported composite steel–concrete beams, and these tests were used by Ranzi et al. (2004) to validate their FE model. Their specimen E1 was used in the present FE analysis. The geometric and material properties of the specimen shown in Fig. 11 were reported by Chapman and Balakrishnan (1964), and were used in the present FE analysis. The beam was subjected to a central concentrated load Q. Variations of the central vertical deflections v_c with the external load Q obtained by the present FE model are compared with the test results in Fig. 12. Four elements were used in the FE analysis. It can be seen that the FE results agree well with the test results. Using their "direct stiffness" FE model Ranzi et al. (2004) also achieved good agreement with these test results.

Simply Supported Composite Beam Tested by McGarraugh and Baldwin

A simply supported steel–concrete composite beam under third-point loading was tested by McGarraugh and Baldwin (1971) and

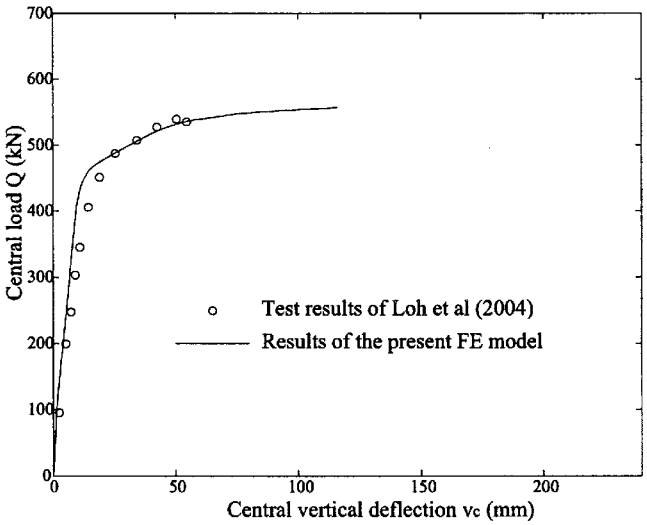

Fig. 17. Comparison with test results for simply supported steel–concrete composite beam of Loh et al. (2004)

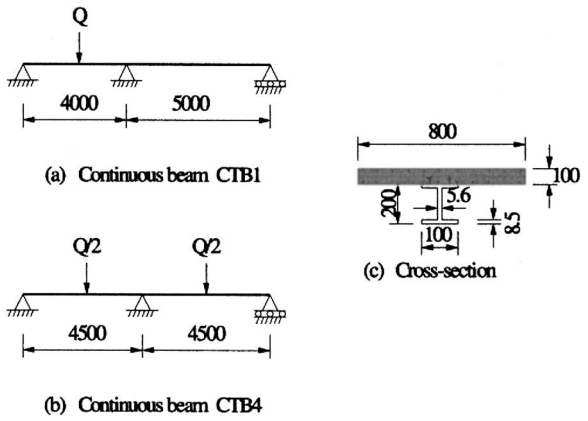

Fig. 18. Continuous steel–concrete composite beams tested by Ansourian (1981)

was used by Ayoub and Fillippou (2000) to demonstrate the efficiency of their mixed formulation of a nonlinear steel–concrete composite beam element. The geometric and material properties of the beam are shown in Fig. 13. However, the Young's modulus of elasticity for steel and concrete, and the strain corresponding to the maximum stress of concrete were not reported. In this investigation, the Young's modulus of elasticity of steel in this North American research was assumed to be E_s=29,000 ksi (200,000 MPa). The Young's modulus of elasticity of concrete was calculated using Eq. (14) with the assumed density of concrete taken as ρ=2,400 kg/m^3. The strain corresponding to the maximum stress of concrete was assumed to be 0.002. The study of Ayoub and Fillippou (2000) showed that the results of their mixed FE model for the load–displacement response agreed very well with the test results, but the results obtained from a FE model based on a displacement formulation either overestimated the response when full composite action was considered or underestimated the response when no composite action was considered.

Variations of the central vertical deflection v_c with the load Q obtained from the present FE model are compared with the experimental results of McGarraugh and Baldwin (1971) in Fig. 14. Eight elements were used in the FE analysis. The agreement between the FE and experimental results is reasonably good.

The distribution of relative slip at the interface between the steel and concrete components at the load level A (shown on Fig. 14) is compared with the test results in Fig. 15. The results of the present FE model somewhat overestimate the measured slip. Ayoub and Fillippou (2000) also reported that the predictions of their mixed and displacement-based FE models overestimated the measured slips although the predictions agree with each other quite well.

Simply Supported Composite Beam in Hogging Bending Tested by Loh, Uy, and Bradford

Eight simply supported composite steel–concrete beams under a central concentrated load were tested by Loh et al. (2004). The test was designed to investigate the behavior of a composite beam in hogging moment regions. The specimen CB1 was used for the present FE analysis. The dimensions of the composite beam and the cross-section properties are shown in Fig. 16. The dimensions of the Australian steel girder 250UB25.7 are: overall depth D=248 mm, flange width b=124 mm, flange thickness t_f=8 mm, and web thickness t_w=5 mm. The thickness of the profiled steel sheeting is t_{prof}=1 mm. Six reinforcement bars of 16 mm diameter were placed at the bottom of the concrete slab with 20 mm cover. A 1,200×100×8 steel plate was used at the flange top of the middle span as the flange stiffener.

The material properties of the composite beam reported by Loh et al. (2004) are as follows:

1. For concrete: Young's modulus of elasticity: E_c=21,500 MPa, the cylinder strength σ_c=26.2 MPa, the strain corresponding to the maximum stress is ϵ_c=0.00337;
2. For reinforcement: Young's modulus of elasticity E_{rein}=194,600 MPa, the proof strength $\sigma_{0.2}$=510 MPa;
3. For profiled steel sheeting: Young's modulus of elasticity E_{prof}=230,900 MPa, proof strength $\sigma_{0.2}$=600 MPa; and
4. For steel girder: Young's modulus E_s=182,400 MPa, yield stress σ_y=315 MPa, ultimate strength σ_u=460 MPa for flanges; while Young's modulus: E_s=207,000 MPa, yield stress σ_y=430 MPa, the ultimate strength σ_u=520 MPa for the web.

In the FE analysis, the strain at which strain hardening starts was assumed to be 11 times the yield strain and the modulus for strain hardening was assumed to be $E_{\tan}$=6,000 MPa for steel girders. Because the flange steel stiffener was located at the top of the flange of the middle span, its role needs to be considered in the FE analysis. The material properties of the flange steel stiffener were not reported, and were thus assumed to be the same as the web of the steel girder.

Variations of the central vertical deflection v_c with the load Q obtained from the present FE model are compared with the experimental results of Loh et al. (2004) in Fig. 17. Eight elements were used in the FE analysis. The agreement between the FE and experimental results is quite reasonable.

Continuous Composite Beam Tested by Ansourian

Six continuous steel-concrete composite beams that are often used as benchmark tests by other researchers were tested by Ansourian (1981). The specimens CTB1 and CTB4 were used to demonstrate the ability of the present FE model in analyzing the nonlinear inelastic behavior of continuous steel–concrete composite beams. The continuous beam CTB1 had two unequal spans and was subjected to a central concentrated load in the short span, while the continuous beam CTB4 had two equal spans and was subjected to equal central concentrated loads at each span as shown in Fig. 18. The dimensions of the cross section are also shown in Fig. 18. The material properties of these two continuous beams are listed in Table 2. The Young's modulus of elasticity of the concrete was not reported. The density of the concrete was

Table 2. Properties of Short CFT Columns Tested by Schneider (1988)

Column	Dimensions (mm×mm)	t (mm)	D/t ratio	L/D ratio	σ_s (MPa)	E_s (MPa)	σ_c (MPa)	E_c (MPa)
S1	127.3×127.3	3.15	40.4	4.8	356	180,518	30.454	26,611
S4	126.8×127.2	7.47	17.0	4.8	347	204,633	23.805	23,528

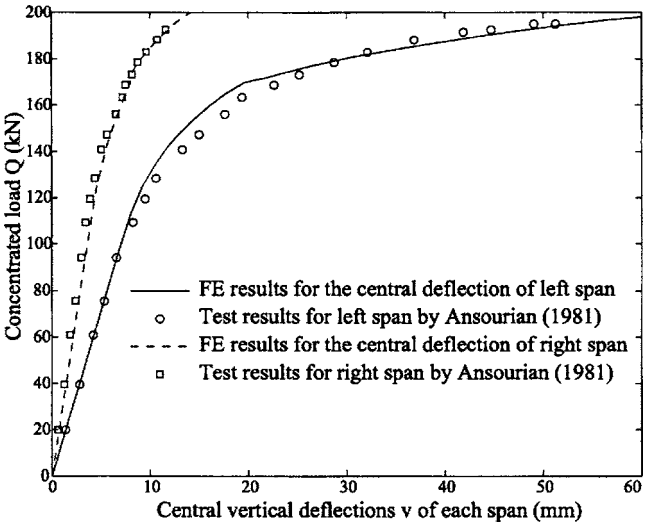

Fig. 19. Comparison with test results for continuous steel–concrete composite beam CTB1 of Ansourian (1981)

used with Eq. (14) to calculate the Young's modulus of elasticity of the concrete for the FE analysis. Because the Young's modulus of elasticity of the steel was not reported, the value of E_s=200,000 MPa was assumed in the FE analysis. Variations of the applied load with the vertical deflections of the middle span are compared with the test results of Ansourian (1981) in Fig. 19 for the beam CTB1 and in Fig. 20 for the beam CTB4. Eight elements were used in the FE analysis for each of the continuous beams. The FE results almost coincide with the test results in both cases.

Conclusions

This paper has described the implementation of the incremental–iterative procedure for the FE model for the second order nonlinear inelastic analysis of composite steel and concrete members. It has been found that using a standard tangent modulus matrix in the incremental–iterative procedure may cause error accumulations which in turn lead to an unsafe drift from the yield surfaces and thus the yield criteria may be violated. Consequently, the quadratic asymptotic rate of convergence of the Newton–Raphson method is lost. To solve this problem, a consistent tangent modulus matrix is needed in the incremental–iteration solution process, and this matrix was described and used.

The implementation of the FE model is flexible. The order of the shape function, the number of the unaxial stress–strain relations, the number of divisions of the cross section, the number of Gaussian points in each division, whether or not including the confinement effects on concrete, and whether or not including the slip between the steel and concrete components in both composite beams, and the CFT columns can be chosen by the user according to the problem at hand.

The application of the FE model to a variety of problems demonstrated the ability of the FE model to predict the nonlinear inelastic behavior of a number of different composite members, including axial compression and uniaxial bending, axial compressive buckling of concrete-filled steel columns, and either simply supported or continuous composite steel–concrete beams. Comparisons with experimental and theoretical results have shown that the FE model provides excellent, effective, and accurate numerical performance.

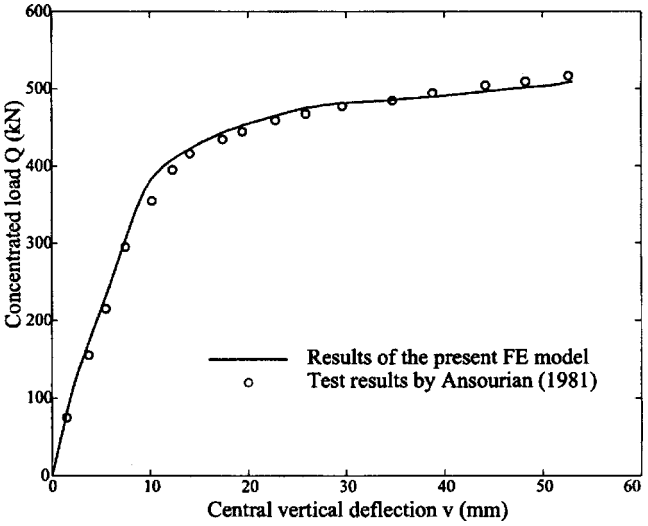

Fig. 20. Comparison with test results for continuous steel–concrete composite beam CTB4 of Ansourian (1981)

Acknowledgments

This work has been supported by an Australian Professorial Fellowship awarded to the second writer, and a Discovery Project awarded to the second and third writers, by the Australian Research Council.

References

Ansourian, P. (1981). "Experiments on continuous composite beams." *Proc., Inst. Civ. Eng.*, 71(2), 25–71.

Ayoub, A., and Fillippou, F. C. (2000). "Mixed formulation of nonlinear steel-concrete composite beam element." *J. Struct. Eng.* 126(3), 371–381.

Bridge, R. Q. (1976). "Concrete filled steel tubular columns." *Civ. Eng. Trans.*, Institution of Engineers, Australia, 18, 127–133,

Chapman, J. C., and Balakrishnan, S. (1964). "Experiments on composite beams." *Struct. Eng.* 42(11), 369–383.

Crisfield, M. A. (1986). "Snap-through and snap-back response in concrete structures and the dangers of underintegration." *Int. J. Numer. Methods Eng.* 22, 751–767.

Gilbert, R. I., and Warner, R. F. (1978). "Tension stiffening in reinforced concrete slabs." *J. Struct. Div. ASCE* 104(12), 1885–1900.

Han, L. H. (2000). "Tests on concrete filled steel tubular columns with high slenderness ratio." *Adv. Struct. Eng.* 3(4), 337–344.

Hu, H. T., Huang, C. S., Wu, M. H., and Wu, Y. M. (2003). "Nonlinear analysis of axially loaded concrete-filled tube columns with confinement effect." *J. Struct. Eng.* 129(10), 1322–1329.

Huang, C. S., et al. (2002). "Axial load behaviour of stiffened concrete-filled steel columns." *J. Struct. Eng.* 128(9), 1222–1230.

Lemaitre, L., and Chaboche, J. -L. (1994). *Mechanics of solid materials*, Cambridge University Press, Cambridge, U.K.

Loh, H. Y., Uy, B., and Bradford, M. A. (2004). "The behaviour of composite beams in hogging moment regions- Part I: Experimental study." *J. Constr. Steel Res.* 60, 897–919.

McGarraugh, J. B., and Baldwin, J. W. (1971). "Lightweight concrete-on-steel composite beams." *Eng. J.* 8(3), 90–98.

O'Brien, A. D., and Rangan, B. V. (1993). "Test on slender tubular steel

columns filled with high strength concrete." *Australian Civil Engineering Trans.*, Institution of Engineers, Australia, CE35(4), 287–292.

Oehlers, D. J., and Bradford, M. A. (1995). "Composite steel and concrete structural members: Fundamental behaviour." Pergamon Press, Oxford, U.K.

Pi, Y.- L., Bradford, B. A., and Uy, B. (2006). "Second order nonlinear inelastic analysis of composite steel-concrete members. I: Theory." *J. Struct. Eng.* 132(5), 751–761.

Ranzi, G., Bradford, M. A., and Uy, B. (2004). "A direct stiffness analysis of composite beams." *Int. J. Numer. Methods Eng.* (in press).

Richart, F. E., Brandtzaeg, A., and Brown, R. L. (1928). "A study of the failure of concrete under combined compressive stresses." *Bulletin 185*, Univ. of Illinois Experimental Station, Champaign, Ill.

Saenz, L. P. (1964). "Discussion of equation for the stress-strain curve of concrete." *J. Am. Concr. Inst.* 61(9), 1227–1239.

Schneider, S. P. (1988). "Axially loaded concrete-filled steel tubes." *J. Struct. Eng.* 124(10), 1125–1138.

Simo, J. C., and Taylor, R. L. (1985). "Consistent tangent operators for rate-independent elastoplasticity." *Comput. Methods Appl. Mech. Eng.* 48(1), 101–118.

Warner, R. F., Rangan, B. V., Hall, A. S., and Faulkes, K. A. (1998). *Concrete structures*, Longman, Melbourne, Australia.

Zienkiewicz, O. C., and Taylor, R. L. (1989). *The finite element method*, 4th Ed., McGraw–Hill, New York.